

Scientific report

regarding the project implementation between January-December 2014

Activity 1.5. Comparison between numerical modeling and experimental results obtained in an experimental model

The geometry used in the numerical modeling consists of a rectangular crucible, $7 \times 7 \times 5 \text{ cm}^3$ in size. The crucible is filled with an eutectic GaInSn alloy. This alloy, because of its low melting point temperature ($\sim 11^\circ\text{C}$) is liquid at room temperature and is usually used as a model fluid in experiments. The material properties used in the numerical modeling are listed in Table 1:

Physical property	Value	Unit
Density, ρ	6360	Kg/m^3
Dynamic viscosity, μ	$2.16 \cdot 10^{-3}$	$\text{N}\cdot\text{s/m}^2$
Electrical conductivity, σ	$3.2 \cdot 10^6$	S/m

Table 1. Material properties of the GaInSn eutectic melt

An electrical current is injected in the melt through two electrodes placed along the diagonal symmetrically from the center point, at $1/3$ and $2/3$ of the diagonal length from the lower left corner, as can be seen from Figure 1.

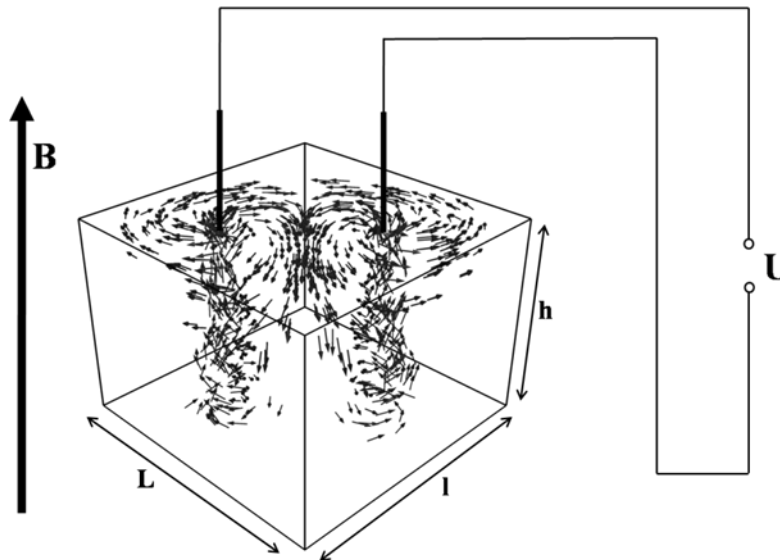


Figure 1. Schematic representation of the numerical model

This set-up is placed in a vertical magnetic field. The combination of the electrical current and the vertical magnetic field generates a Lorentz force which gives a rotational flow component to the fluid convection.

To study the influence of the electromagnetic field on the melt convection for each value of the magnetic field ($B = 5, 10, 20, 30 \text{ mT}$) a range of electrical current intensities ($I = 0.1, 0.5, 1, 2, 5, 10, 15, 20, 25, 30, 35, 40, 45 \text{ A}$) was considered in our simulations. In order to obtain a realistic solution

500 s in real time were computed with a time step of 0.1 s, for each combination of I and B . On the last 300 s a time averaged solution was computed (in order to compare the velocity profiles with the ones measured from the experiment). The 3D time-dependent simulations were performed on a BlueGene/P supercomputer at the HPC Center, West University of Timisoara using a parallelized version of STHAMAS3D.

Experimental model

In order to validate the numerical results, a model experiment was devised. A rectangular shaped glass crucible of $7 \times 7 \times 7 \text{ cm}^3$ in size, containing an eutectic GaInSn melt is placed inside the air gap of an electromagnet. The continuous current C shaped electromagnet was designed in order to obtain a stationary and nearly uniform magnetic field in the air gap. As in the numerical simulations, the total volume of the melt is $7 \times 7 \times 5 \text{ cm}^3$, with the top surface of the melt being uncovered. Two electrodes, fixed in a lid covering the crucible, touch the GaInSn free melt surface. They are placed along the diagonal symmetrically from the center at $1/3$ and $2/3$ of the diagonal length (Figure 2). In order to minimize the effects on the thermal and velocity fields at the free surface, two hemispherical tipped cylindrical electrodes immersed in the melt immediately below the cylindrical part (the half sphere has a 2 mm radius) were employed for this study. A continuous electrical current passes through the electrodes into the melt, causing an electromagnetic stirring effect in conjunction with the applied magnetic field.

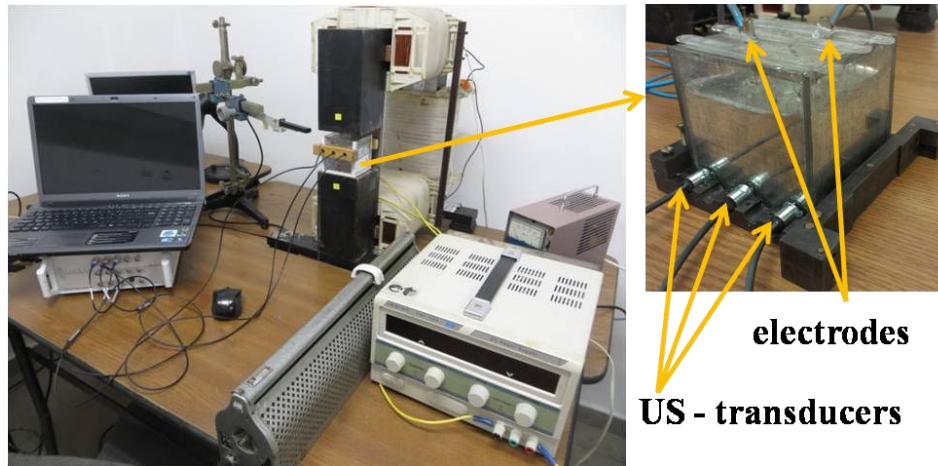


Figure 2. Experimental installation of C-shape EM with air gap, where the crucible is placed; ultrasonic transducers in connection with DOP3010 Velocimeter are fitted perpendicular to the crucible side

The maximum self-magnetic field generated by a hemispherical electrode for the highest value of the electrical current used in the experiment, 5A, and a hemisphere radius of about 2 mm, is [1]:

$$B_{\text{self}} = \frac{\mu_0 I}{2\pi R} = 0.5 \text{ mT}$$

This value can be considered negligible in respect to the magnetic fields considered in this present study, which vary between 5 and 30 mT. Thus the effect of this extra magnetic field was not considered in the numerical simulations.

In order to measure velocity profiles, the UDV technique was employed, by using the commercial measurement system DOP3010 from Signal Processing S.A., which was successfully used in flow measurements in liquid metals [2]. The UDV method used in DOP3010 is based on the pulse-echo technique, allowing visualization of velocity profiles along the propagation direction of the ultrasonic waves inside the flowing liquid by auto-correlating the different ultrasonic echoes received after the emission of a series of repetitive pulses. The ultrasonic signal comes from particles suspended in the liquid that are present in the path of the ultrasonic beam. These particles need to have different acoustic impedance than the fluid environment. In the case of GaInSn, the gallium oxide particles formed at the free melt surface are the source of the reflected ultrasound. The improvement of the ultrasonic signal was obtained at the beginning of the experiment by carefully mixing the oxide from the surface inside the melt. The velocity was averaged over a period of 1200 s of measuring time from the experimental profiles.

Three 4 MHz ultrasonic (US) transducer probes were used. The transducers have been positioned perpendicular to the outside wall of the crucible held by a support (see Figure 2). Ultrasonic coupling between the sensors and the glass wall was realized through the use of a standard ultrasonic gel. These sensors were put in three positions (left, middle, right) along a horizontal line. The transducers, which are perpendicular to the crucible wall, measure the velocity component perpendicular to the wall, which by convention is negative if the flow is oriented towards the transducer and positive if the flow is directed away from it. A measurement volume is defined laterally by the ultrasonic beam divergence and axially by the sampling bandwidth, which has to correspond to a length longer than the emitted pulse. For these measurements, the axial dimension of the sampling volume is 2.184 mm. The resolution between two points is given by the distance between the centers of two consecutive measurement volumes. The measurement volumes overlap, as the distance between the centers of two volumes is about 10 times smaller than their axial length. The transducers contain a 5 mm diameter piezoelement, giving approximately the initial diameter of the ultrasonic beam in the near field region which diverges up to about 9.5 mm at 7 cm in depth. Therefore, the considered position of the transducer will be the one corresponding to its central axis. The velocity profile is thus averaged around the axis of the transducer, which is always described by a set of x and z coordinates.

For this measurement technique, all the profiles usually have biased values or present measurement artifacts in the near field region (about 10 mm for a GaInSn melt at 4.130 MHz, for a cylindrical transducer with a diameter of 5 mm).

Results

Numerical simulations of electromagnetic stirring in a square isothermal crucible

The numerical simulations of the electromagnetic stirring of a GaInSn melt inside a rectangular crucible show that the flow structure is dependent on the values of electrical current I passing through the electrodes and applied magnetic field B . For a symmetrical electrode positioning along the diagonal of the melt free surface, two main structures have been observed, that appear to dominate the fluid flow. These types of structures can be better observed for the extreme values of electrical current at the different applied magnetic fields, as can be seen in Figure 3. Flow lines were illustrated, using Paraview software, through particle tracking from two flow sources placed at the top (blue color) and bottom (red color) ends of the vortex structure. The radial component of the electrical current combined

with the vertical magnetic field gives rise to a Lorentz force distribution causing a rotational motion of the melt. Due to a converging meridional flow generated by a radial pressure gradient the rotational movement is concentrated towards the center into an ascending vortex type structure [3]. This type of structure is well known in the literature [1], [4-6].

The flow spiraling from one electrode intersects with the opposing flow (in the radial direction) coming from the other electrode. The resulting flow is channeled along the diagonal between the electrodes and turns downwards at the top corner and then again at the bottom corner, as can be seen in Figure 3. We named this flow a poloidal recirculation.

For small values of I , up to 2 A depending on the magnetic field, the swirling vortex that appears below each electrode is stronger than the poloidal recirculation and is extending down to the bottom of the crucible (Figure 3 (a), (c)). In this case, the vortices are connecting all the flow in the poloidal direction.

For high values of I , from 2 A to 25 A depending on the magnetic field, the flow structure changes. The poloidal recirculation becomes stronger and splits the vortex below each electrode into two vortices localized at the top and bottom ends of the crucible (Figure 3 (b), (d)). The poloidal recirculation is connecting the two vortices formed around the electrodes (in blue), and is collecting the flow originating from the vortices at the bottom (in red).

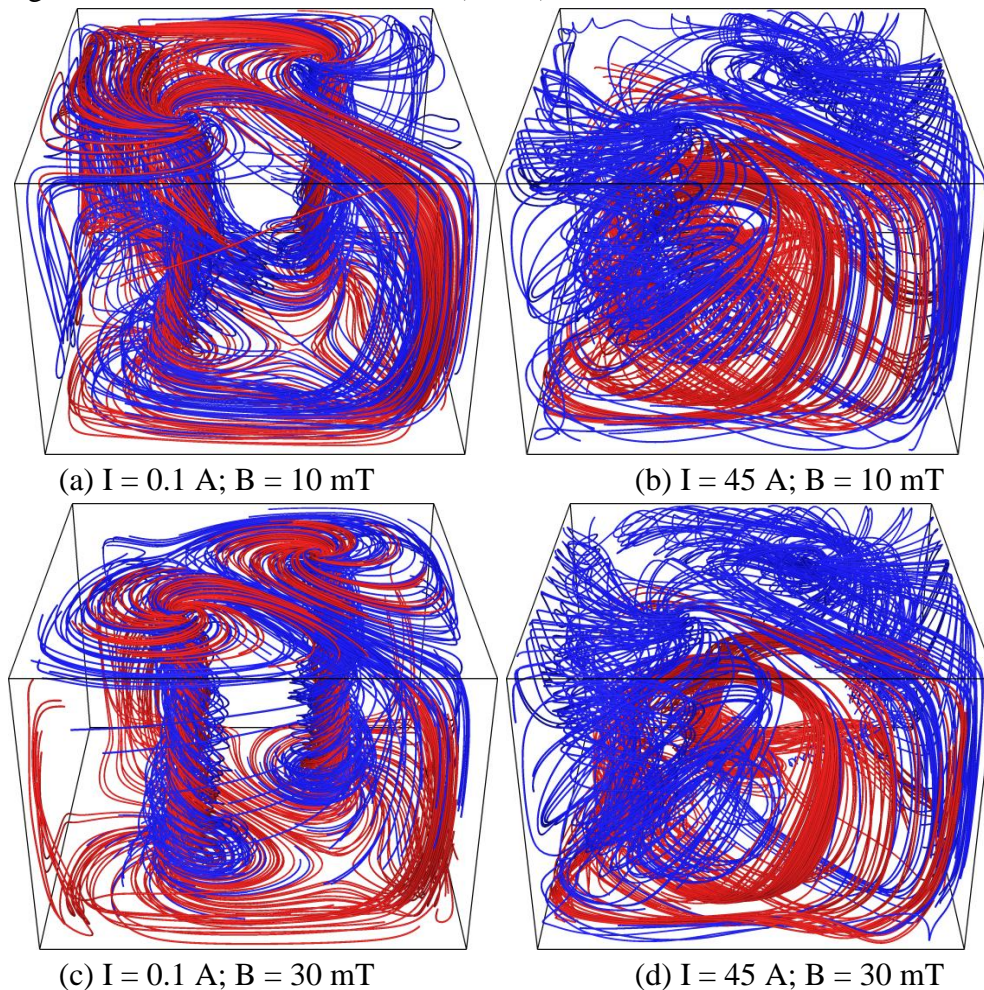


Figure 3. Particle tracking of flow structure for different electrical current I and magnetic field B pairs

For simplicity, we shall refer to the first structure described here as a "Vortex" structure, due to the vortex flow component domination and to the second one as a "Poloidal" one, due to the dominance of the poloidal flow component.

For a more detailed description of the phenomena giving rise to the different structures, due to the symmetry of the flow, we will examine the flow around only one electrode, which is represented in Figure 4 for a given magnetic field induction ($B = 30$ mT). Because of the perspective of this view, the interaction between the vortex structure and the poloidal recirculation is emphasized. In Figure 4(a), we can see the vortex domination case. Close to the bottom of the crucible, the poloidal flow interacts with the opposing vortex dominated flow in the position marked by a dark arrow. In the case from Figure 4(a), a clear vortex type structure can be found below the electrode and the poloidal flow is absorbed into the vortex in the upward direction. As the electrical current intensity increases, the poloidal flow intensity increases too and the vortex structure is gradually deformed (Figure 4(b) and (c)). In these transition cases towards a poloidal dominant flow, the vortex absorbs just a part of the poloidal recirculation. Finally, for high enough electric current values (e.g. $I = 45$ A), a "Poloidal" structure is obtained (Figure 4(d)). In this case the vortex structure is split into two vortices one near the surface and one near the bottom. The poloidal flow now absorbs both vortices and connects them through a complex recirculation.

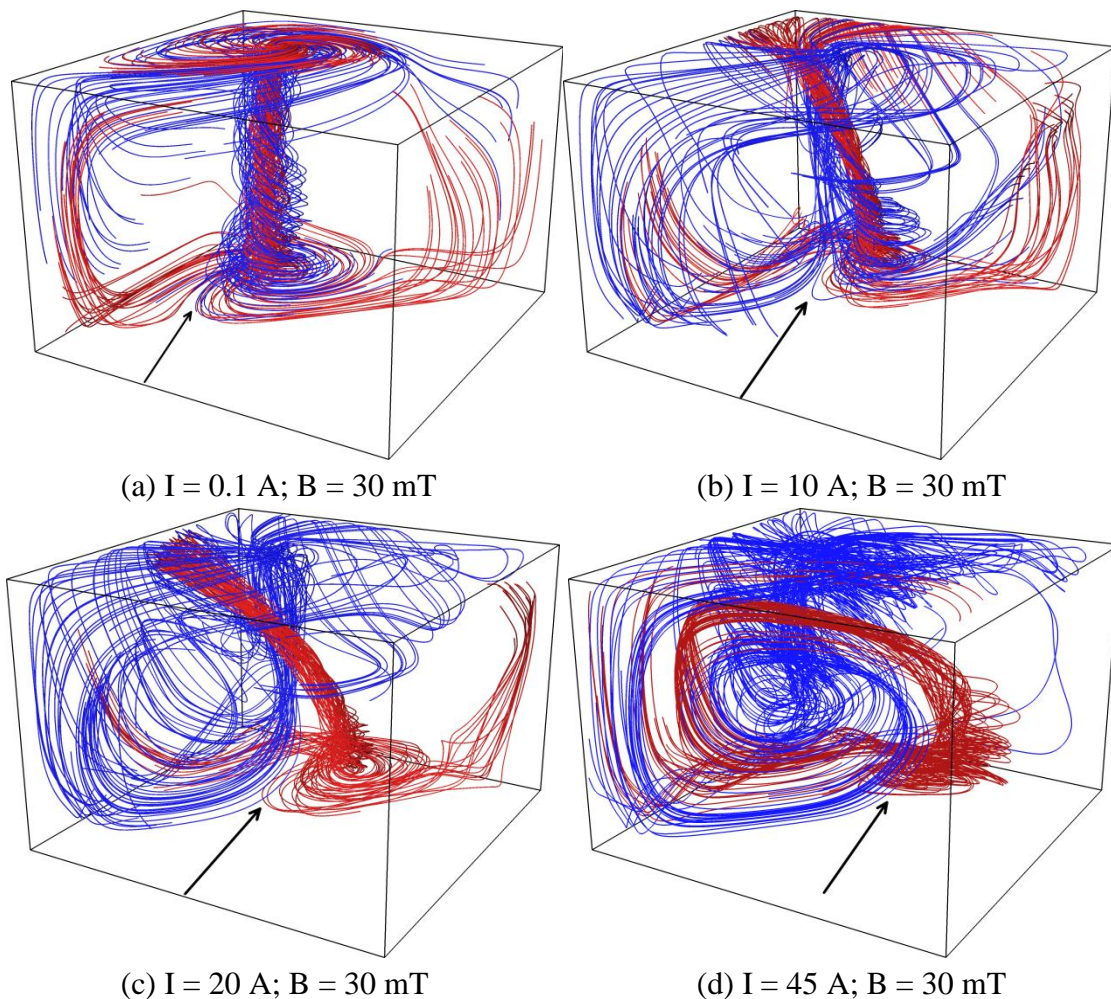


Figure 4. Particle tracking of flow structure for different electrical current I and magnetic field B pairs

In order to characterize the interaction between the "Vortex" and the "Poloidal" flow structures, we will consider the distance along the diagonal where the two opposing flows balance at the bottom, marked by a dark arrow in Figure 4. In a horizontal plane at 5 mm height from the bottom (Figure 5), we can clearly see the position on the diagonal where this balance between the flow structures is attained. We can therefore define a parameter L_{struct} as a characteristic length corresponding to the flow structure.

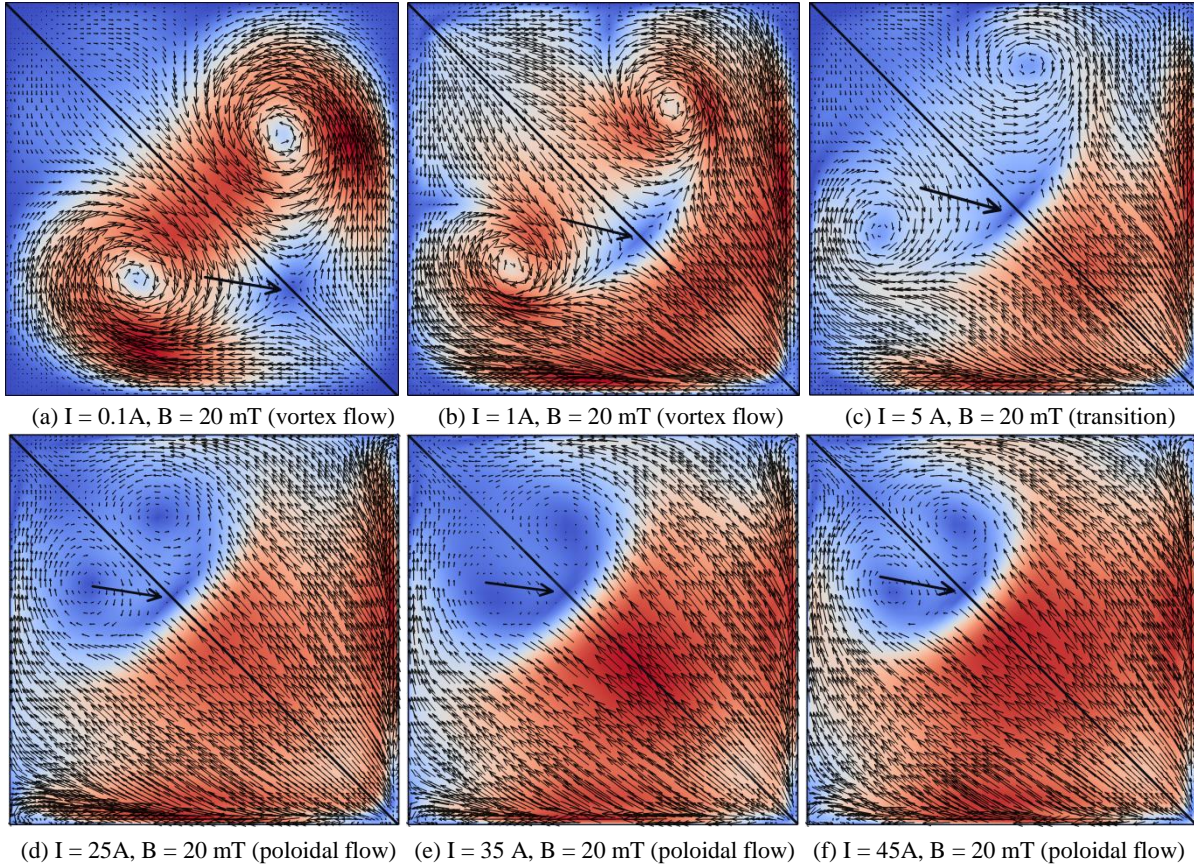


Figure 5. Flow structure in the plane simulated for different electrical currents I (0.1 A – 45 A) and a magnetic field $B = 20$ mT at 5 mm from the crucible base. The arrow represents the place of balance between the opposing vortex driven and poloidal flows. The colors represent the velocity magnitude (red - high velocity; blue - low velocity)

In Figure 6, L_{struct} was plotted for the electrical currents and magnetic fields used in simulations. Each simulation result was analyzed in accordance with the criteria for identifying the flow structure type ("Vortex", "Poloidal" or transition) presented above.

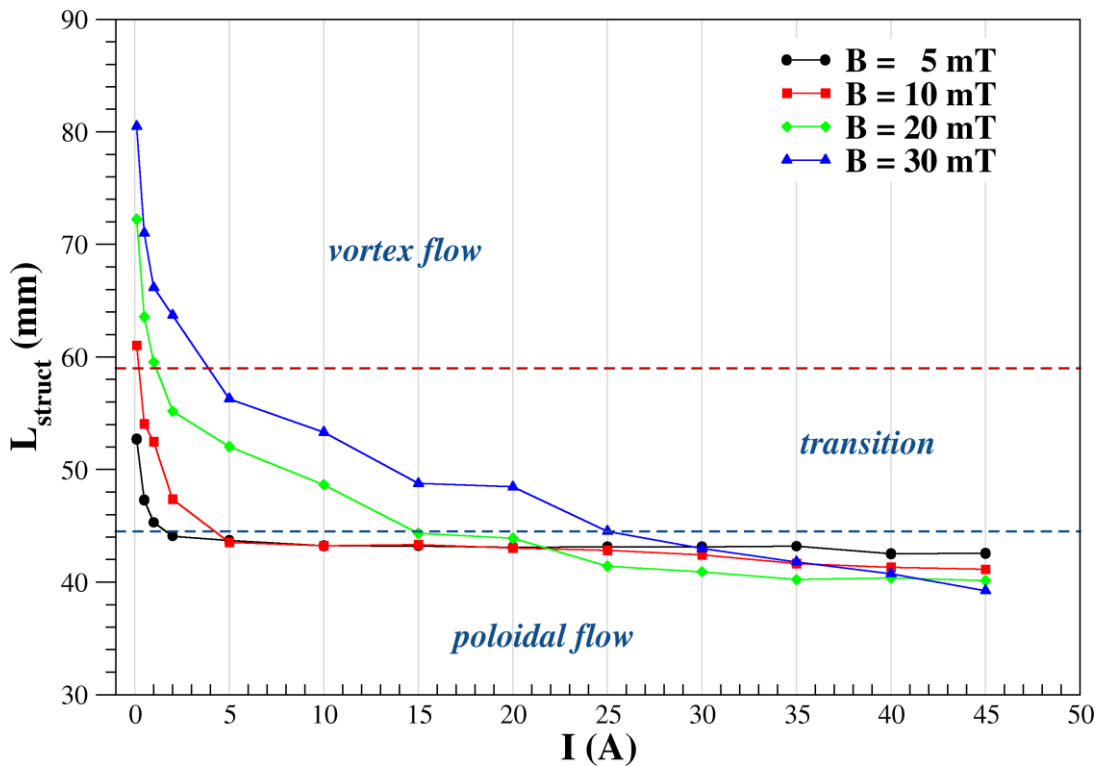


Figure 6. L_{struct} as a characteristic length defining the “Vortex” to “Poloidal” structure transition for the different electrical currents I and magnetic fields B that have been numerically simulated

From Figure 5 one can observe that, close to the crucible bottom, where the position of the crystallization interface should be in the case of DS, the distribution of higher flow velocities (in red) is wider and more uniform for the "Poloidal" cases than the "Vortex" ones. Also, the areas where the melt is very poorly mixed (or "dead" flow areas, with very low velocities, represented in dark blue) are more narrowly distributed and concentrated towards one corner, decreasing in size with the increase of current intensity I for a given B . It may be concluded that a "Poloidal" flow structure type of EMF melt mixing will lead to a lower rate of precipitate formation than a "Vortex" flow structure.

Validation of the numerical method by the model experiment

To validate the existence of the flow structures predicted by the numerical simulations, experimental UDV profiles were acquired as near as possible to the plane where the "Vortex" to "Poloidal" structures transition was quantified. The centers of the US transducers piezoelements were positioned as low as possible from the bottom, at $z = 6$ mm from the base of the crucible, because of the relative difference between the crucible bottom and the transducer support height. Their x coordinate positions, from the left side of the crucible were: left - 8.5 mm; middle - 35.5 mm; right - 62.5 mm. The experimental profiles were compared on the same chart with velocity profiles taken along the Oy direction from the numerical simulations from the same x and z positions as the transducers axes positions.

Figure 7(a) shows a comparison between numerical and experimental results for a "Vortex" structure, obtained at 2 A and 30 mT, while Figure 7(b) shows a comparison between numerical model and experiment for a "Poloidal" structure, obtained at 5 A and 5 mT. The "Vortex" case shows that the shape of the velocity profiles is the same in the numerical model and in the experiment, which denotes

the same flow structure. For the “Poloidal” case, the shape of the velocity profiles is slightly different in experiment and simulation, with a greater difference for the left transducer, which denotes comparable flow structure. A greater difference in the “Poloidal” case is expected due to high three-dimensional complexity of the flow. In both cases, the velocity values are greater in the experiment than in the simulation.

The differences may arise from the experimental uncertainties like deviations from the no-slip condition on the container boundaries, area of the electrodes contact to the melt, divergence of the ultrasonic beam, imprecision in the electromagnetic parameters values determination (due to current oscillations or small inhomogeneity of the magnetic field) or the inaccuracy of the material constants values used in the numerical model.

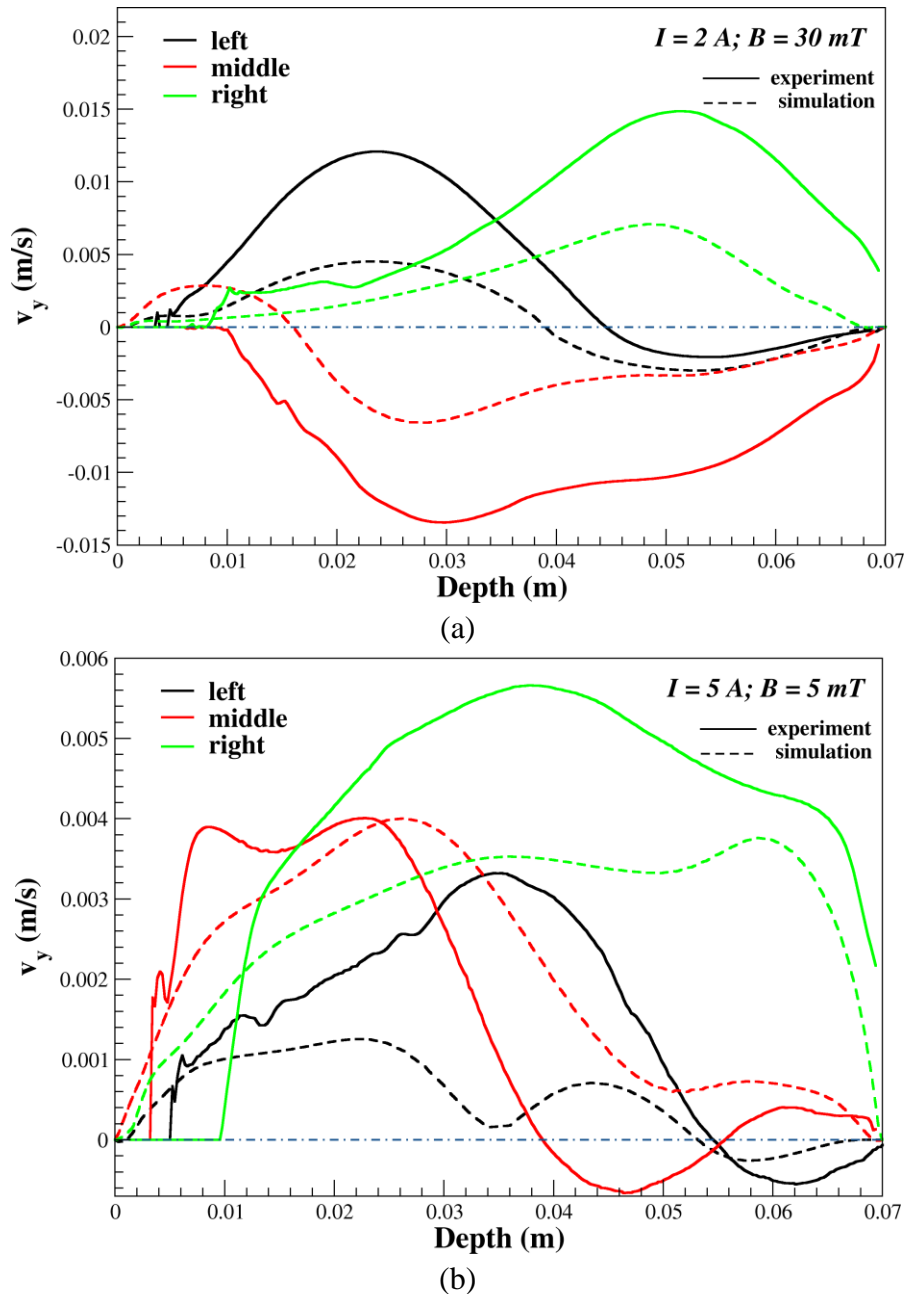


Figure 7. Experimental and numerical time-averaged velocity profiles for each of the three transducers (denoted as left, middle, right) at: (a) $I = 2 \text{ A}$ and $B = 30 \text{ mT}$; (b) $I = 5 \text{ A}$ and $B = 5 \text{ mT}$

References:

- [1] V. Bojarevics, Ya. Freibergs, E. I. Shilova, E. V. Shcherbinin, *Electrically Induced Vortical Flows*, Kluwer Academic Publishers, 1989, pp. 6, 174-195.
- [2] A. Cramer, C. Zhang and S. Eckert, Local flow structures in liquid metals measured by ultrasonic Doppler velocimetry, *Flow Measurement and Instrumentation* 15 (2004), 145-153.
- [3] T. Vogt, I. Grants, S. Eckert, G. Gerbeth, Spin-up of a magnetically driven tornado-like vortex, *Journal of Fluid Mechanics* 736 (2013), 641-662.
- [4] R. Moreau, *Magnetohydrodynamics*, Springer, Dordrecht, 1990, ch. 6, pp. 211-217.
- [5] P. A. Davidson, J. C. R. Hunt, Swirling recirculating flow in a liquid-metal column generated by a rotating magnetic field, *Journal of Fluid Mechanics* 185 (1987), 67-106.
- [6] P. A. Davidson, The interaction between swirling and recirculating velocity components in unsteady, inviscid flow, *Journal of Fluid Mechanics* 209 (1989), 35-55.

Activity 3.1. Numerical modeling for melt convection and interface shape in a industrial scale set-up for different values of the magnetic field and electrical current using 2 and 4 electrodes

In this study a rectangle crucible with a 7 cm square base and a height of 5 cm is used. The crucible is filled up with an eutectic alloy of GaInSn chosen because it's liquid at room temperature and it's dynamic viscosity and electrical conductivity have similar values with silicon. Therefore it is frequently used in model experiments.

An electrical current is injected in the melt through four electrodes placed at the melt free surface. The four electrodes are placed along the two diagonals, very close to the crucible boundaries as can be seen from Figure 1.

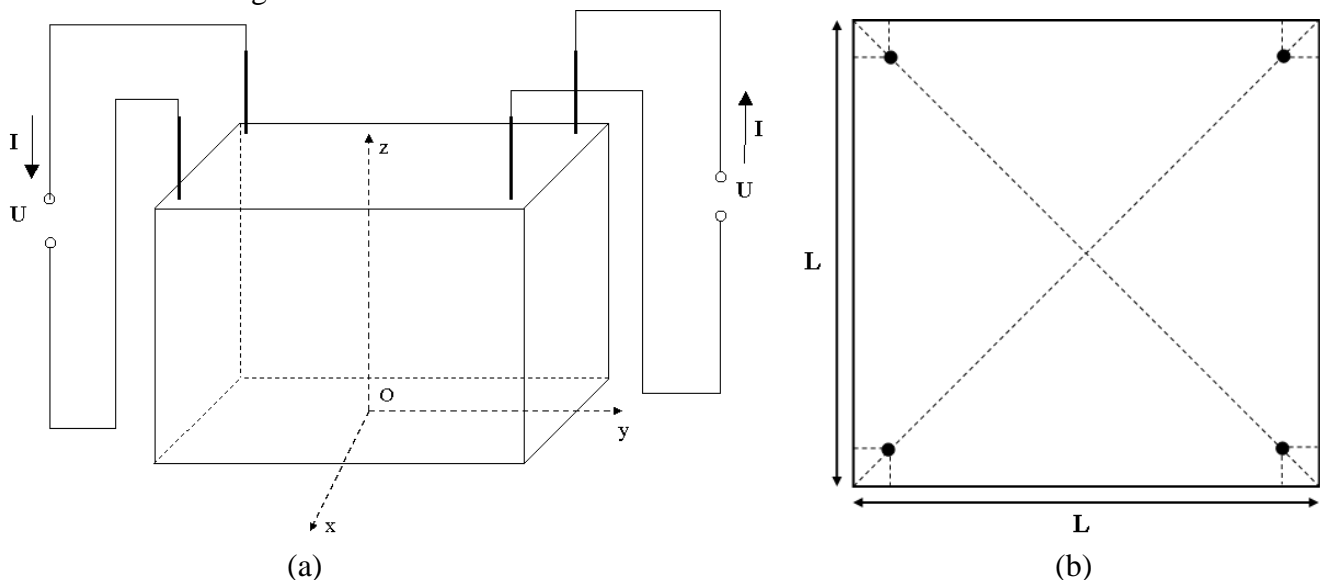


Figure 1. (a) Schematic representation of the four electrodes numerical model used in the numerical modeling (b) the four electrodes arrangement at the melt free surface.

The electrical current is injected in the circuit through two power supplies so that through the two electrodes placed along the first diagonal the electrical current goes into the melt and the circuit is

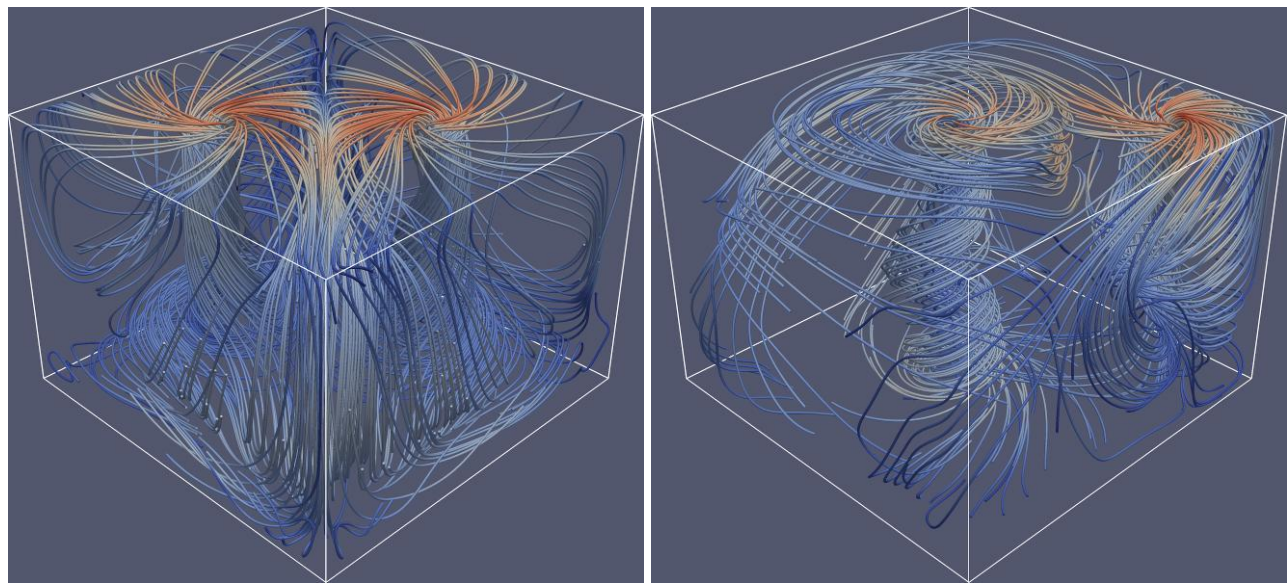
closed through the other two. The experimental set-up is then placed in a vertical magnetic field. The combination between the electrical current and the magnetic field induces a Lorentz force that generates a melt rotation.

The studies made on a two electrodes configuration either symmetrically or asymmetrically arranged indicated the appearance of poloidal or vortex type structures depending on the electrical current intensities of magnetic field induction. These structures lead to a better mixing of the whole melt, but there are still some area where the melt is stationary. In order to try to avoid the appearance of these "dead areas" in the melt four electrodes were used.

In the numerical modeling three values for the electrical current intensity, between 10 and 40 A were considered. The magnetic field induction is fixed at 30 mT. The numerical simulation were done with the STHAMAS3D software and 1000 s in real time were simulated.

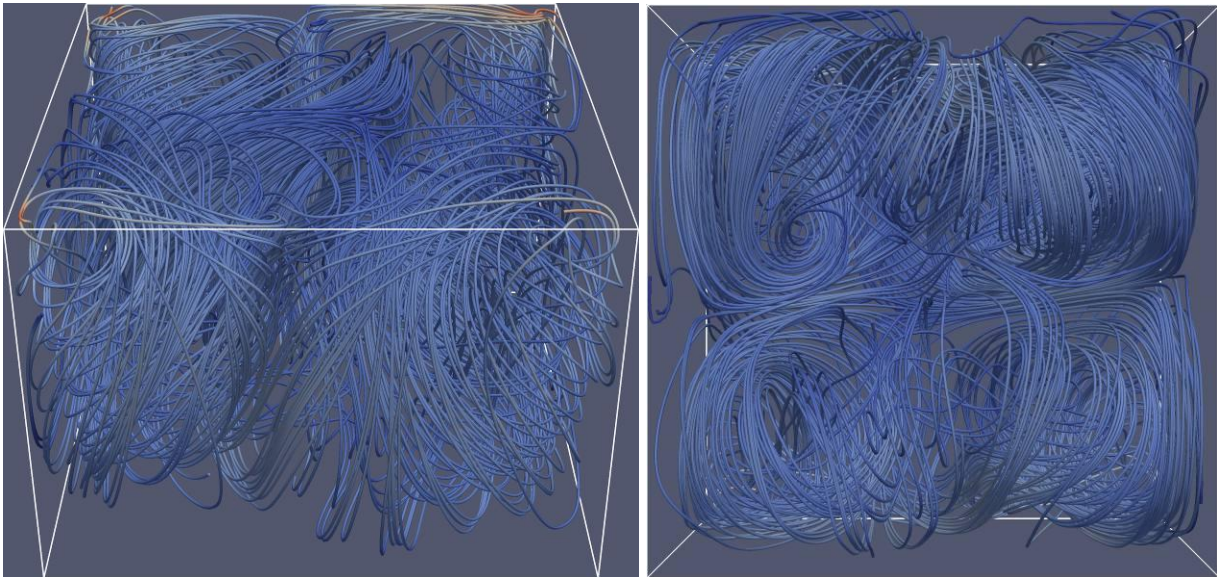
For the numerical modeling made with two electrodes it can be seen that, for an intensity of 10 A, two vortices centered around each electrode (Figure 2 (a),(b)). For the symmetrical configuration (SC), the two vortices start at the melt free surface intersecting close to the bottom of the crucible. In the case of the asymmetrical configuration (AC) of the electrodes a central vortex appears that acts on the whole melt length from the free surface to the crucible bottom. It is also observed the appearance of a vortex around the electrode placed near the crucible boundary, it's action being fairly limited, the melt rotation being dominated by the central vortex (Figure 2 (b)).

For the four electrodes configuration, in the case of $I=10$ A and $B=30$ mT four convection structures (tilted vortices) are observed generated by the four electrodes (Figure 2(c)). Similar to the poloidal structure observed in the case with two electrodes, a vortex starts from each electrode it's rotation axis being tilted diagonally. The vortices corresponding to the electrodes on each side are joined together in the melt center, their rotation going in the meridional plane gradually. Therefore, two poloidal structures are formed, one on the side corresponding to the electrodes connected to one power supply and the other on the side corresponding to the electrodes connected to the other power supply. The two structures intersect in the center of the melt which leads to a better melt mixing. These structures can be observed from the bottom view of the crucible (Figure 2(d)). They appear as two convection rolls symmetrical to the median line of the crucible bottom. In the case of a directional solidification configuration, these convection rolls would carry the impurities accumulated near the solid-liquid interface, thus better mixing them in the melt.



(a) Two symmetrical electrodes

(b) Two asymmetrical electrodes



(c) Four electrodes

(d) Four electrodes, bottom view

Figure 2. Melt flow for $I = 10$ A; $B = 30$ for different electrodes positions

As the electrical current intensity increases, it can be seen that for a symmetrical configuration of the two electrodes appears a transition towards the poloidal structure, the two vortices starting from the melt free surface intersect on the radial direction much closer to the melt free surface (Figure 3(a)). For the asymmetrical configuration (Figure 3(b)), the central vortex still dominates the melt rotation, but the intensity of the vortex centered in the electrode placed closer to the crucible corner increases. The flow structure becomes much more complex for the four electrodes configuration (Figure 3(c),(d) and Figure 4(a),(b)) the four vortices joining together near the melt free surface forming two poloidal structures that intersect each other along the diagonal line that contains the electrodes through which the electrical current is injected into the melt.

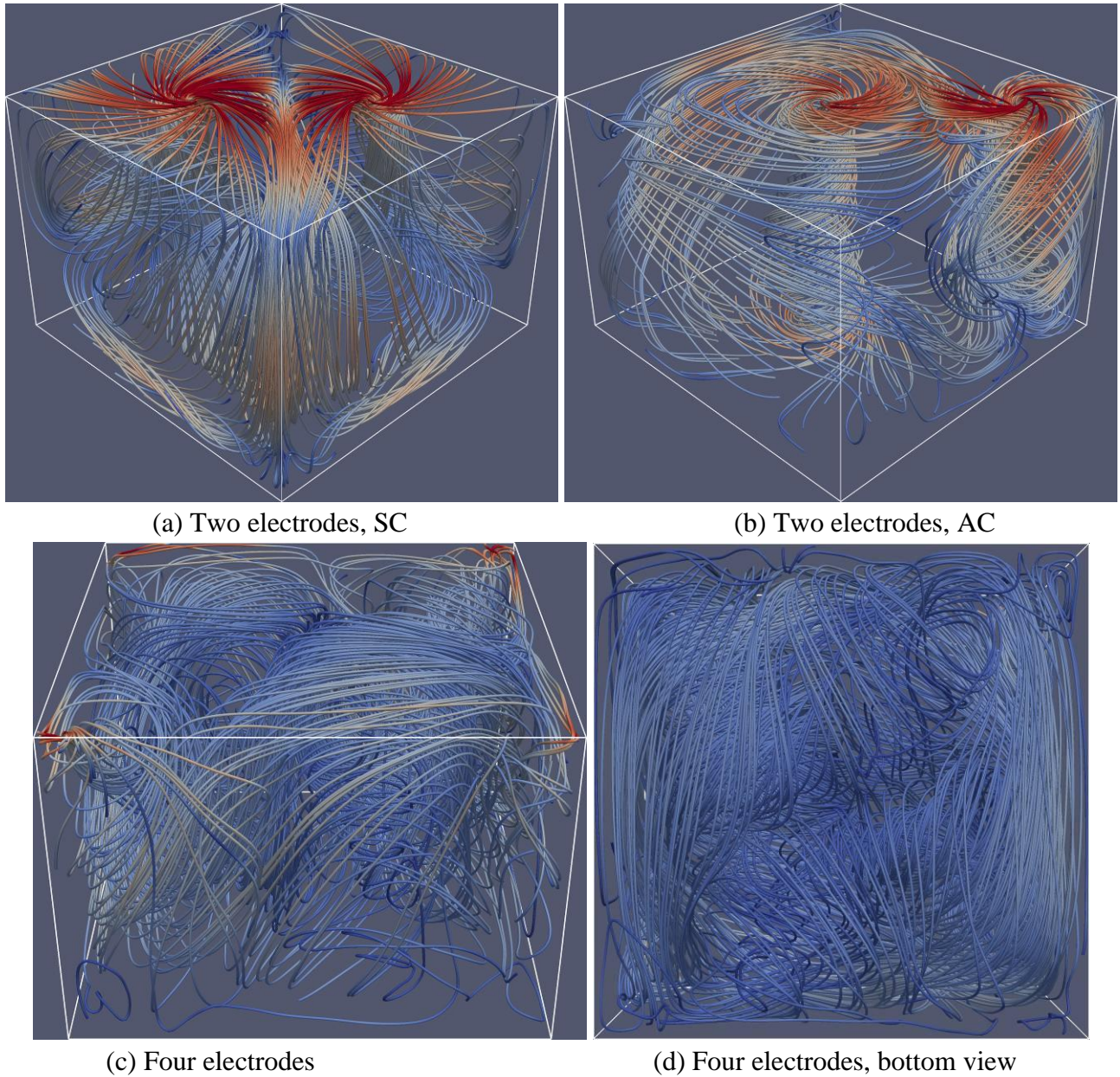


Figure 3. Melt flow for $I=20A$, $B=30$ mT for different electrodes position at the melt free surface

The two loops move on a poloidal direction towards the bottom of the crucible, where they collect the accumulated impurities, and returning to the melt free surface along the crucible walls. In this case, from the bottom of the crucible these structures are observed as two convection rolls (Figures 3(d) and 4(b)) with a symmetry shifted from the meridional line to the diagonal of the crucible bottom. From the bottom view it can be observed that even the melt in the corners is set in motion thus avoiding an accumulation of unwanted impurities on the crucible edges in the case of a directional solidification configuration.

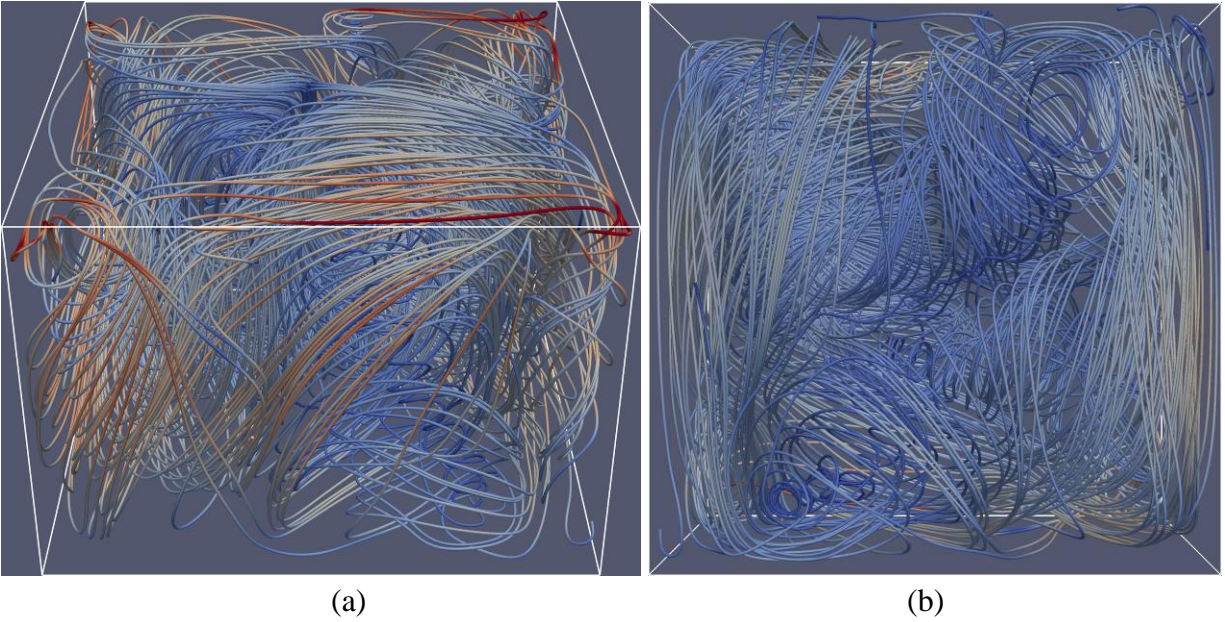


Figure 4. Melt flow for $I=40A$, $B=30$ mT in the case of 4 electrodes configuration: (a) general view; (b) bottom view

From Table 1 it can be seen that the maximal flow velocity increases if the rotational movement is generated by four electrodes. Therefore, comparing with the cases where the electrical current is injected into the melt through two electrodes, either symmetrical or asymmetrical configured, the maximal flow velocity is at least two times higher for all studied cases. The maximal flow velocity are much higher in the case of the four electrodes configuration because the melt homogenization doesn't require such a long period of time.

Electrode configuration	I (A)	B (mT)	v_{max} (m/s)
2 electrodes; SC	10	30	0.05
	20	30	0.073
	40	30	0.107
2 electrodes; AC	10	30	0.046
	20	30	0.066
	40	30	0.0956
4 electrodes	10	30	0.131
	20	30	0.185
	40	30	0.264

Table 1. Maximal velocity of the melt flow for different electrodes configurations

Dissemination:

Articles:

1. Numerical and experimental modelling of melt flow in a directional solidification configuration under the combined influence of electrical current and magnetic field, R. Negrila, A. Popescu, D.Vizman, European Journal of Mechanics B/Fluids, submitted

Conferences:

1. Radu Negrila, Alexandra Popescu, Daniel Vizman - *Novel electromagnetic stirring technique in a direct-solidification configuration*, E-MRS 2014 Spring Meeting, Lille, France, 27-29 May 2014
2. Radu Andrei Negrila, Alexandra Popescu, Marius Paulescu, Daniel Vizman - *Control of convective flows in a rectangular crucible by a special type of electromagnetical stirring*, 9th PAMIR International Conference, Fundamental and Applied MHD, Riga, Latvia, 16-20 June 2014
3. Radu Andrei Negrila, Alexandra Popescu, Bogdan Barvinschi, Marius Paulescu, Daniel Vizman - *GaInSn melt flow structure variation with crucible size in an isothermal electromagnetic stirring configuration*, TIM14 Physics Conference, Timisoara, Romania, 20-22 November 2014

Project manager,
Prof. Dr. Daniel Vizman